Diagn Interv Radiol 2025; DOI: 10.4274/dir.2025.253283

ABDOMINAL IMAGING

ORIGINAL ARTICLE

Readout-segmented echo-planar imaging and conventional single-shot echo-planar imaging for determining cervical cancer image quality, lymphovascular space invasion, and lymph node metastasis status: a comparative study

Huizhen Song[1,2]
Jiao Bai[2]
Yu Wang[2]
Juan Xie[2]
Yunzhu Wu[3]
Jian Shu[2,4]

[1]Chengdu Seventh People's Hospital (Affiliated Cancer Hospital of Chengdu Medical College), Department of Radiology, Chengdu, China

[2]The Affiliated Hospital of Southwest Medical University, Department of Radiology, Luzhou, China

[3]Nanjing University of Information Science and Technology, School of Artificial Intelligence, AI in Medicine, Nanjing, China

[4]Medical Imaging Key Laboratory of Sichuan Province, North Sichuan Medical College, Nanchong, China

Corresponding author: Jian Shu

E-mail: shujiannc@163.com

Received 21 February 2025; revision requested 05 April 2025; accepted 05 May 2025.

Epub: 23.06.2025

Publication date: 06.11.2025

DOI: 10.4274/dir.2025.253283

PURPOSE

Diffusion-weighted imaging (DWI) using single-shot echo-planar imaging (ss-EPI) is prone to artifacts, geometric distortion, and T2* blurring. Readout-segmented echo-planar imaging (rs-EPI) may improve image quality in the DWI of cervical cancer (CC). This study aimed to compare the image quality between rs-EPI and ss-EPI DWI in CC and to evaluate whether the apparent diffusion coefficient (ADC) values of ss-EPI (ssADC) and rs-EPI (rsADC) can differentiate the status of lymphovascular space invasion (LVSI) and lymph node metastasis (LNM).

METHODS

This prospective study included 69 patients with CC who underwent ss-EPI and rs-EPI DWI before surgery. Qualitative reader scores, signal-to-noise ratio (SNR), contrast-to-noise ratio (CNR), and ADC values derived from ss-EPI and rs-EPI were compared. The differences in ADC values were analyzed in patients who were (a) LNM-positive (LNM+, n = 17) and LNM-negative (LNM–, n = 52); (b) LVSI-positive (LVSI+, n = 33) and LVSI-negative (LVSI–, n = 36).

RESULTS

The rs-EPIs of CC had higher subjective image quality scores and a lower SNR than ss-EPI (all $P < 0.001$); no significant differences existed between rs-EPI and ss-EPI for either CNR or ADC (CNR, $P = 0.313$; ADC, $P = 0.949$; $P > 0.05$ for all). The rsADC and ssADC of the LNM+ group were substantially lower than those of the LNM– group (rsADC, $P = 0.000$; ssADC, $P = 0.000$; $P < 0.001$ for all); the areas under the receiver operating characteristic curve were 0.855 and 0.851, respectively. However, there were no differences in ADC values between the LVSI+ and LVSI– groups (rsADC, $P = 0.271$; ssADC, $P = 0.200$; $P > 0.05$ for all).

CONCLUSION

Over a similar scan time, rs-EPI improves the qualitative image quality of DWI significantly more than ss-EPI and has good diagnostic accuracy for LNM status in CC. However, neither could predict the LVSI status.

CLINICAL SIGNIFICANCE

Readout-segmented EPI improves the qualitative image quality of DWI and has good diagnostic accuracy for LNM status in CC, compared with conventional ss-EPI. It is more inclined to qualitative analysis of CC foci and provides a better scheme when choosing the DWI sequence scanning strategy for CC.

KEYWORDS

Echo-planar imaging, cervical cancer, signal-to-noise ratio, diffusion-weighted imaging, lymphovascular space invasion, lymph node metastasis

You may cite this article as: Song H, Bai J, Wang Y, Xie J, Wu Y, Shu J. Readout-segmented echo-planar imaging and conventional single-shot echo-planar imaging for determining cervical cancer image quality, lymphovascular space invasion, and lymph node metastasis status: a comparative study. *Diagn Interv Radiol.* 2025;31(6):539-546.

Despite its extensive screening programs, cervical cancer (CC) remains the fourth most common cancer among women worldwide.[1] Lymphovascular space invasion (LVSI) refers to the presence of tumor cells in the lymphatic vessels and/or within the blood vessels. Although not involved in CC staging, it can predict lymph node metastasis (LNM) and is used as an independent prognostic factor for recurrence and survival.[2,3] The latest International Federation of Gynecology and Obstetrics 2018 staging system noted that the treatment efficacy of stage IB2 and stage IIA1 early CC surgery and chemoradiation is consistent, and the National Comprehensive Cancer Network Clinical Practice Guidelines in Oncology recommends that patients with LNM classified as stage IIIC cancer, who are candidates for external beam radiation therapy, undergo brachytherapy and chemotherapy instead of surgical procedures.[3,4] If the risk factors for LNM and LVSI are identified after surgery, adjuvant chemoradiotherapy needs to be further strengthened. However, combined surgery and chemoradiotherapy is associated with increased adverse effects and greater complications.[5] Accurate evaluation of the LVSI and LNM before surgery can reduce the complications of both surgery and chemoradiation, avoid excessive surgery, and prevent depriving young women of childbirth.

Around the edges of the tumor focus are functional lymphatic channels, along which the primary tumor spreads to the regional lymph nodes.[6] The peripheral tumor tissue between the tumor and normal tissues is rich in tumor stem cells and likely to determine tumor invasiveness.[7] However, the anterior bladder and posterior gas-containing rectum are challenging anatomical regions, making cervical diffusion-weighted imaging (DWI) at 3.0T magnetic resonance (MR) susceptible to artifacts and geometric distortion, especially in these tumor marginal areas. The conventional sequence used for DWI–single-shot echo-planar imaging (ss-EPI)–has various limitations that may induce geometric distortion, T2 blurring effect, and susceptibility to artifacts.[8] Through shortening the echo time (TE) and echo spacing along the k-space readout trajectory, readout-segmented echo-planar imaging (rs-EPI) DWI sequences may overcome these shortcomings.[9,10]

This study compares the subjective and objective image quality of rs-EPI and ss-EPI in CC and determines the feasibility and effectiveness of the marginal area apparent diffusion coefficient (ADC) values from ss-EPI and/or rs-EPI for evaluating the invasive status of the tumor into the lymphovascular space and lymph nodes in patients with CC.

Main points

- The anterior bladder and posterior gas-containing rectum are challenging anatomical regions, making cervical diffusion-weighted imaging (DWI) at 3.0T magnetic resonance susceptible to artifacts, geometric distortion, and T2* blurring, especially in cervical cancer (CC) marginal areas.
- Readout-segmented echo-planar imaging (rs-EPI) DWI can produce clear anatomic details and reduce ghost artifacts and distortion in DWI of CC, achieving higher subjective and qualitative diagnostic value.
- No difference was found between rs-EPI and single-shot echo-planar imaging (ss-EPI) with respect to apparent diffusion coefficient values pertaining to the edges of CC lesions.
- rs-EPI and ss-EPI had similar good diagnostic accuracy in the prediction of lymph node metastasis status in CC.

Methods

Patients

This study was approved by the Institutional Ethics Committee of The Affiliated Hospital of Southwest Medical University, and informed consent was obtained from all the patients (May 2021; decision number of the ethics committee approval: KY2021-04101). A total of 130 consecutive female patients with pathologically diagnosed CC underwent an MR examination and subsequent surgery as primary surgery at the hospital between June 2021 and March 2023. The MR imaging (MRI) examination included ss-EPI DWI and rs-EPI DWI. Of the patients initially included in the study, 46 were excluded due to the following criteria: 1) history of preoperative therapy (neoadjuvant chemotherapy, radiotherapy, or conization) (n = 36); 2) incomplete histopathological data (n = 7); 3) the diameter of each lesion was <1 cm on the MRI (n = 15); 4) rare histological types of CC (big cell neuroendocrine carcinoma, clear cell carcinoma) (n = 3). The remaining 69 cases were finally divided into an LVSI+ versus LVSI- patients' group and an LNM+ versus LNM- patients' group, respectively. The inclusion and exclusion criteria are summarized in Figure 1.

Magnetic resonance imaging protocols

The MR examinations were performed on a 3T MR scanner (MAGNETOM Prisma, Siemens Healthineers, Forchheim, Germany). Conventional MRI was acquired, including the following sequences: axial and sagittal T2W imaging [repetition time (TR)/TE, 4,000/89 ms]; axial contrast-enhanced T1W imaging with fat saturation (TR/TE, 600/10 ms). Before injecting the contrast agent, ss-EPI and rs-EPI DWI were performed with comparable imaging parameters (Table 1). Patients who were menstruating or had an intrauterine device in the uterine cavity at the time of MRI acquisition were excluded.

Qualitative evaluation of image quality

All database analyses were performed on a workstation (Syngo.via; Siemens Healthineers). Qualitative image evaluation was performed by two independent radiologists (reader 1: BZ, with 8 years of experience;

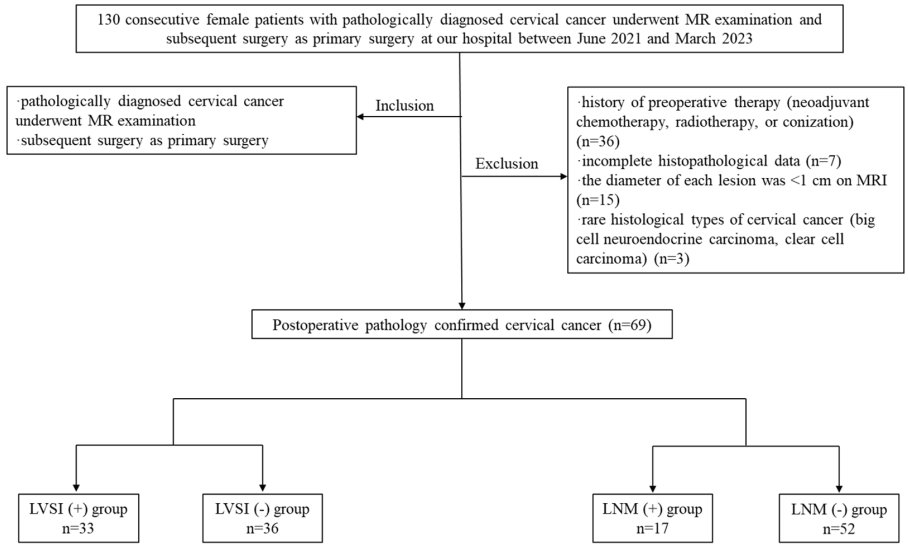

Figure 1. Flowchart showing the inclusion and exclusion criteria for patient selection. LVSI, lymphovascular space invasion; LNM, lymph node metastasis; MRI, magnetic resonance imaging.

reader 2: JC, with 15 years of experience) who were blinded to the corresponding DWI scanning sequence parameters. The two observers anonymized and randomly distributed all DWI parameters. Taking axial and sagittal T2W images and axial contrast-enhanced T1W images as a reference, the image anatomical details, geometric distortion and ghosting artifacts, lesion conspicuity, and overall image quality were assessed using a 5-point scale (1 = non-diagnostic, 2 = poor, 3 = general, 4 = good, 5 = excellent) according to the research by Zhang et al.[11]

Quantitative evaluation of images

The quantitative analysis included the measurement of the signal-to-noise ratio (SNR), CNR, and ADC values. All regions of interest (ROIs) were manually delineated by a radiologist (FW) who had 20 years of experience involving pelvic MRI. Lesion ROIs were placed on axial oblique DWIs with a b-value of 800 s/mm^2 guided by T2W images and contrast-enhanced T1W images. An irregular lesion ROI included the tumor edge on the biggest image slice, which encompassed the peripheral area within a 5-10-mm radius of the edge of high-intensity tumors and avoided obvious necrotic, higher signal artifacts and deformation areas. Background and tissue ROIs were selected as a circular drawing with an area of approximately 5 mm^2. All ROIs were measured twice, and the average was calculated. In the results, signal $(S)_{lesion}$ is the mean signal intensity inside the lesion ROI, standard deviation $(SD)_{background}$ is the standard deviation of the background noise ROI, S_{tissue} depicts the mean signal intensity of the musculus glutaeus medius tissue ROI, and SD_{lesion} and SD_{tissue} represent the standard deviation of the lesion ROI and musculus glutaeus medius tissue ROI, respectively.

Next, a well-matched copy of the cervical lesion ROI was generated automatically at the corresponding location of each ADC image. An example of a cervical lesion ROI acquired on rs-EPI is shown in Figure 2 (b = 800 s/mm^2).

Statistical analysis

Statistical analysis was performed using SPSS, version 25.0 and MedCalc, version 15.2.2. A two-tailed *P* value of <0.05 was considered statistically significant for all analyses. Regarding subjective image quality, intra-observer agreement was assessed using kappa statistics. The kappa values were in the range of 0–1.00 and interpreted as follows: 0.40 = poor; 0.41–0.60 = moderate; 0.61–0.80 = good; >0.81 = excellent.[12] The qualitative parameters (reader score) between the two DWI protocols were compared using the Wilcoxon signed-rank test. The Shapiro–Wilk test was conducted to assess the normal distribution of all continuous variables. The quantitative parameters (SNR, CNR, ADC) were compared between ss-EPI and rs-EPI using the paired Student's t-test (when conforming to a normal distribution) or the Wilcoxon signed rank test. The consistency of ADC values between ss-EPI and rs-EPI was estimated using the intraclass correlation (ICC) coefficient with a two-way analysis of variance with a random-effects model. An ICC of 0.75–1.00 indicated excellent agreement, 0.60–0.74 good agreement, 0.40–0.59 fair agreement, and <0.4 poor agreement.[13]

For further analysis, differences in ADC values were analyzed between (a) the LNM+ and LNM– groups and (b) LVSI+ and LVSI– using Student's t-test (when data were normally distributed) or the Mann–Whitney test. The diagnostic performance of the two ADC values was described by receiver operating characteristic (ROC) analysis. The area under the ROC curve (AUC) values were also calculated, and the DeLong test was used to compare the differences among the AUCs.

Table 1. Imaging parameters for ss-EPI and rs-EPI sequences

Parameters	ss-EPI	rs-EPI
Diffusion mode	Three-scan trace	Three-scan trace
Parallel imaging	GRAPPA	GRAPPA
Fat-suppressed	Fat sat; strong	Fat sat; strong
TR (ms)	6,400	6,400
TE (ms)	65	53
Partial fourier	0.625	0.625
Field of view (mm × mm)	320 × 320	320 × 320
Matrix	160 × 160	160 × 160
Number of slices	25	25
Slice thickness (mm)	3	3
Intersection gap (%)	20	20
Phase-encoding direction	Anteroposterior	Anteroposterior
Echo spacing (ms)	0.64	0.32
Bandwidth (Hz/Px)	2,840	925
EPI factor	136	113
Number of readout segments	1	5
b-value (s/mm^2)	50, 800	50, 800
Average	1, 5	1, 1
Scan time (min:sec)	2:20	2:18

ss-EPI, single-shot echo-planar imaging; rs-EPI, readout-segmented echo-planar imaging; GRAPPA, generalized autocalibrating partially parallel acquisition; TR, repetition time; TE, echo time.

Results

Patient characteristics

A total of 69 patients (mean age: 47.5 years; age range: 31–66 years) with CC were enrolled in this retrospective study. Of these, 17/52 patients were staged as LNM+/LNM–; in the LNM+ group, the lymph node size was <10 mm for all patients. Among all patients, 33/36 patients were staged as LVSI+/LVSI– according to the pathological findings. Table 2 shows the demographic characteristics of patients recruited in this study.

Comparison of subjective visual scores

Comparisons of the rs-EPI and ss-EPI quality based on a 5-point scoring system are shown in Table 3. Intra-observer agreement of the anatomic structure, artifacts and distortion, lesion conspicuity, and overall imaging quality were good or excellent in two DWI sequences (kappa statistics: ss-EPI 0.777, 0.726, 0.883, 0.787; rs-EPI 0.731, 0.879, 0.692, 0.705). For both readers, the rs-EPI group achieved significantly better scores in each aspect than the ss-EPI group (all $P < 0.001$, Table 3). Examples of rs-EPI advantages are presented in Figure 3.

Comparison of quantitative image quality

The mean and standard deviation of CNR and SNR are listed in Table 4. The SNR value of the rs-EPI was lower than that of the ss-EPI DWI (445.28 ± 107.33 vs. 138.60 ± 47.80, *P* <

Figure 2. Plots **(a-d)** show the schematic of drawing a CC lesion region of interest (ROI). **(a)** In the sagittal T2W image, the red dashed line region is the biggest image slice depicting cancer foci; **(b)** single-shot echo-planar imaging diffusion-weighted image with b-values of 800 s/mm^2 with an irregular ROI; **(c)** the corresponding apparent diffusion coefficient image with the ROI from **(b)**; **(d)** the corresponding axial contrast-enhanced T1W image. CC, cervical cancer.

Table 2. Patient characteristics

Characteristics	Patients	
Total number	69	
Age (years)	47.5 (31–66)	
Histological subtype	n	%
Squamous cell carcinoma	62	89.86
Adenocarcinoma	7	10.14
FIGO stage (2018)		
IB	32	46.38
IIA	20	28.99
°C	17	24.64
LNM status		
LNM+	17	24.64
LNM-	52	75.36
LVSI status		
LVSI+	33	47.83
LVSI-	36	52.17

FIGO, International Federation of Gynecology and Obstetrics 2018; LNM, lymph node metastasis; LVSI, lymphovascular space invasion.

0.001). In terms of CNR, there was no significant difference between the ss-EPI and rs-EPI (5.11 ± 1.55 vs. 4.89 ± 1.60, $P = 0.313$).

Diffusion-weighted imaging quantitative parameters

There was no significant difference between the ADC values for ss-EPI and rs-EPI DWI ($P = 0.949$, Table 4). The consistencies of ADC values between ss-EPI and rs-EPI were in complete agreement (ICC: 0.886, $P < 0.001$). Table 5 shows the ADC values corresponding to LVSI and LNM. In both ss-EPI and rs-EPI DWI, the ADC value of ss-EPI (ssADC) and that of rs-EPI (rsADC) were significantly lower in the LNM+ group than in the LNM- group ($P = 0.000$, 0.000, respectively), and there were no significant differences in the ssADC and rsADC values between the LVSI+ and LVSI- groups ($P = 0.271$, 0.200, respectively).

The results of the ROC analyses for ADC values used to distinguish LNM+ from LNM– are shown in Figure 4 and Table 5. The mean AUCs were 0.851 for ssADC and 0.855 for rsADC, and there was no significant difference between the two AUCs (DeLong test: $Z = 0.871$, $P = 0.163$).

Discussion

Comparison of image quality between readout-segmented echo-planar imaging and single-shot echo-planar imaging

The echo spacing of rs-EPI was reduced to 0.32 ms compared with 0.64 ms for ss-EPI in this study. Intra-reader agreement of subjective visual estimation evaluated using kappa was good or excellent, which confirmed the reliability of the investigation, and we demonstrated that the anatomic detail, ghosting artifacts, geometric distortion, and lesion conspicuity of CC DWI based on rs-EPI were significantly superior to ss-EPI. This is consistent with previous findings from abdomen pelvic research, which confirmed improved subjective visual assessments of image quality in rs-EPI for CC, endometrial carcinoma, rectal cancer, renal cancer, pelvic cancer, and sacroiliitis.[10,11,14-17] However, the quantitative image quality (SNR, CNR) of rs-EPI was not satisfactory. We found that the SNR on rs-EPI was significantly lower than on ss-EPI, which is consistent with previous studies.[18-22] No significant difference in the CNR of rs-EPI and ss-EPI was observed, which agrees with previous studies.[18,20-22]

The evaluation of the objective image quality between rs-EPI and ss-EPI continues to be a controversial topic. As the SNR depends to a large extent on the specific protocol followed, we adjusted the two DWI technique parameters of TR values, fields of view, matrices, slice thicknesses, and gaps to coincide for the facilitation of the quantitative comparison. Theoretically, a shorter TE results in an increased SNR. In principle, the shortened TE of rs-EPI was not enough to offset the increase in the SNR caused by

Table 3. Comparison of qualitative parameters between ss-EPI and rs-EPI

Parameters	Reader 1			Reader 2		
	ss-EPI mean ± SD	rs-EPI mean ± SD	*P* value	ss-EPI mean ± SD	rs-EPI mean ± SD	*P* value
Anatomic structure	3.12 ± 0.54	4.43 ± 0.58	<0.001	3.33 ± 0.63	4.47 ± 0.61	<0.001
Artifacts and distortion	3.06 ± 0.38	4.65 ± 0.48	<0.001	3.08 ± 0.34	4.61 ± 0.57	<0.001
Lesion conspicuity	3.71 ± 0.50	4.22 ± 0.77	<0.001	3.73 ± 0.53	4.27 ± 0.76	<0.001
Overall imaging quality	3.45 ± 0.50	4.41 ± 0.64	<0.001	3.35 ± 0.48	4.45 ± 0.50	<0.001

ss-EPI, single-shot echo-planar imaging; rs-EPI, readout-segmented echo-planar imaging; SD, standard deviation.

the increase in the ss-EPI average number to 5. Through setting the scanning parameters, we contribute to the similar scanning time of the two techniques (2 min 20 s vs. 2 min 18 s). We found that such imaging parameter settings and the results reached were similar to previous studies.[18-22] Recently, most images from rs-EPI tend to have higher SNRs and CNRs than the images from ss-EPI but with the expense of a comparatively longer scan time. However, in clinical practice, saving scanning time is an important task considering the numerous MR examinations performed daily. In the present study, the similar short scanning time of the two techniques (2 min 20 s vs. 2 min 18 s), under the premise of reasonable lower SNR of rs-EPI, was not representative of decreased definition or image quality; the SNR and CNR only refer to a part of the quantitative index of the image quality. rs-EPI technology mainly helps achieve higher resolution and reduces susceptibility artifacts and T2* blurring compared with ss-EPI technology. Under the premise of reasonable SNR and CNR, we need rs-EPI DWIs with these visual advantages to improve the accuracy of the early assessment of CC lesions.

In addition, the simultaneous multi-slice (SMS) acquisition scheme may be a potential solution to ensure a higher SNR and CNR while taking a shorter scan time. Instead of a consecutive excitation, the SMS technique concurrently excites multiple slices to decrease scan time.[23] This method has been successfully applied to MRI scanning of the kidney, liver, pancreas, breast, and rectum.[24-28] In the future, we will investigate the combination of SMS and readout-segmented techniques for cervix uteri DWI.

Application of apparent diffusion coefficient in the study of cervical cancer

In this study, rs-EPI showed clearer anatomical details, fewer artifacts and deformation, and higher lesion conspicuity; furthermore, the focal edge ROI outlined on the corresponding DWI truly reflected the tumor edge. We found that the ADC values obtained using ss-EPI and rs-EPI were not significantly different. As previously reported, the new DWI technique did not affect ADC quantification; the ADC values of rs-EPI DWI were as reliable as conventional ss-EPI but with better image quality.[14,17,29,30] Only a few studies found the opposite result; Wisner's study on breast tumors revealed that within benign lesions, malignant lesions, and normal tissue, the mean ADC measurements were lower with rs-EPI than with ss-EPI.[14] According to the authors, this was due to T2* blurring on rs-EPI. However, Xu et al.[21] and Zhao et al.[22] considered the distortion and artifacts of ss-EPIs to be a more reasonable explanation, as no adjacent normal tissue with high ADC value could be found in the sinonasal or orbital region. In the present study, drawing an irregular ROI avoided obvious necrotic, higher signal artifacts and deformation areas on ADC maps of CC, which may explain the lack of differences in ADC values between rs-EPI and ss-EPI DWI sequences.

This study also found that 17 cases eventually developed lymph node metastases and were finally classified as stage °C, and their lymph node size was <10 mm. In general, node size is the MRI criterion in

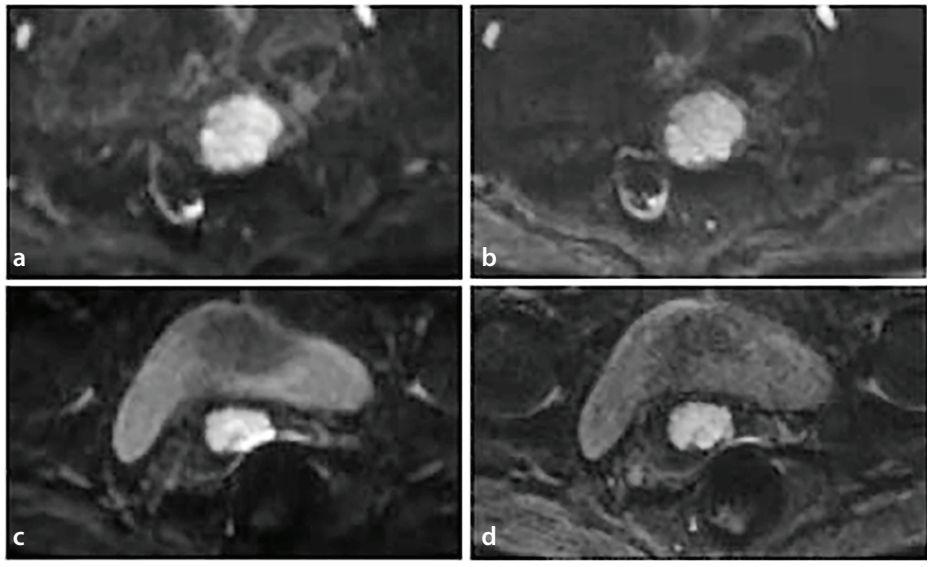

Figure 3. Plots **(a, b)** show a 51-year-old woman with cervical cancer (CC); **(a)** the single-shot echo-planar imaging (ss-EPI) shows blurred anatomical details and a diffusion-restricted lesion with blurred edges, making it unclear whether the lesion broke the outer edge of the cervical wall; **(b)** distinct boundary between the rectum, uterus, and diffusion-restricted lesion in readout-segmented echo-planar imaging (rs-EPIs). Plots **(c, d)** show a 54-year-old woman with CC; **(c)** ss-EPI demonstrating obvious artifacts shown as significantly enhanced local signal and evident distortion between the rectum and lesion; **(d)** minor artifacts and distortion in rs-EPIs.

Table 4. Comparison of quantitative parameters between ss-EPI and rs-EPI

Parameter	ss-EPI mean ± SD	rs-EPI mean ± SD	t value	*P* value
SNR	445.28 ± 107.33	138.60 ± 47.80	22.749	<0.001
CNR	5.11 ± 1.55	4.89 ± 1.60	1.016	0.313
ADC ($\times 10^{-3}$ mm^2/s)	1.01 ± 0.17	1.02 ± 0.17	-0.064	0.949

SNR, signal to noise ratio; CNR, contrast to noise ratio; ADC, apparent diffusion coefficient; ss-EPI, single-shot echo-planar imaging; rs-EPI, readout-segmented echo-planar imaging; SD, standard deviation.

distinguishing lymphatic metastasis from non-lymphatic metastasis; the threshold diameter is 10 mm in the short axis.[31] However, the size of metastatic, hyperplastic, and normal lymph nodes can overlap, and the small lymph nodes could undergo micro-metastases.[32] Williams et al.[33] verified via histological analysis that 54.5% of metastatic nodes were <10 mm in patients with gynecologic malignancy. Clearly, the assessment of lymph node size alone increased the false-negative rate of LNM. In the present study, the inclusion criteria included surgical radical treatment that was abandoned due to suspected LNM based on imaging findings. Specifically, cases with irregular lymph node morphology or a short axis diameter >10 mm on MRI were excluded. In essence, the 17 cases of lymph node metastases that were missed by MRI and not confirmed as positive by LNM exhibited more subtle pathological significance that is not readily apparent to the naked eye. The measured ADC values in these cases can more accurately reflect the internal tumor cell proliferation and tumor aggressiveness within the lesion. This suggests potential value in differentiating ADC values between the LNM+ and LNM- cases. Although the number of lymph node-positive cases was limited to 17, this sample size remains statistically acceptable for analysis.

We validated that both marginal region rsADC and ssADC values of CC could predict lymph node metastatic status (P = 0.000, 0.000, respectively), in agreement with a previous study;[34] both rsADC and ssADC values had a good diagnostic efficacy (AUC: 0.855, 0.851, respectively). In addition, neither of these two ADC values could distinguish the LVSI status of CC, in agreement with previous studies.[35,36] LVSI-positive lesion tumors are characterized by their high invasiveness and a complex microenvironment, which includes an increased density of cancer cells, a high nuclear-cytoplasmic ratio, and reduced extracellular space. Additionally, the vascular blood flow within these tumors is marked by high perfusion. These features collectively illustrate the biological characteristics of tumor heterogeneity. The ADC value serves as a quantifier for the degree of diffusion movement of water molecules, which correlates with cell density in biological tissues. However, it is important to note that, in contrast to cell density, the vascular properties of tumors exert an opposing influence on ADC values, highlighting the distinct physical and biological differences between diffusion and perfusion in tumor tissues;[37] in other words, the heterogeneous ADC values are insufficient for evaluating the LVSI+ status in CC. Even with the higher image quality of rs-EPI, identifying the LVSI status using the ADC from the tumor edge region remains challenging. Nevertheless, a study by Yang et al.[38] concluded that minimum-ADC values could predict LVSI in CC; the ROI of the tumor location was plotted layer by layer on DWIs, with a total of 20–30 ROIs placed (40–50 mm^2), ultimately selecting the ROI with the smallest ADC value. Yang et al.[38] explained that minimum-ADC values reflect a higher density of tumor cells, which may be more sensitive to tumor proliferation. Therefore, minimum ADC values could serve as a feasible and objective parameter to reduce ADC variability. In contrast, Cheng et al.[39] investigated the value of ADC histogram analysis based on whole tumor volume for the preoperative prediction of LVSI. The conclusion drawn is that ADCmax, ADCrange, ADC90, ADC95, and ADC99 were significantly lower in the LVSI+ group than in the LVSI– group (all P values <0.05). This finding may be related to the inclusion of hemorrhagic, necrotic, and cystic regions in the volume of interest (VOI). It is evident that different ADC-derived parameters exhibit variations in their ability to identify LVSI, which depend on the heterogeneity represented in the measured ADCs and are closely related to the ROI or VOI. The original intention of our study was to use the tumor margin area, which is prone to artifacts, as the monitoring reference point. The obtained value represented an average ADC value of the margin area, differing from the ADC measurement values of various regions within the tumor or the ADC histogram of the entire tumor volume.

DWI improves uterine tumor detection and characterization and the visualization of small implants in peritoneal carcinomatosis.[40] To improve the accuracy of a qualitative assessment of CC, such as judging parametrial invasion, DWIs should be included.[41] On this basis, the present study found that advantage should be taken of the higher image quality of rs-EPI, as it is, to some extent, more inclined to the subjective and qualitative judgment of CC, providing a better choice for making DWI sequences in the future.

This study has several limitations. First, some cervical tumors with small lesion diameters (<10 mm) were excluded because of insufficient image pixels for analysis. Analyses of advanced CC (stages IIB–IVA) were also limited because most patients with advanced CC were excluded from concurrent chemo-

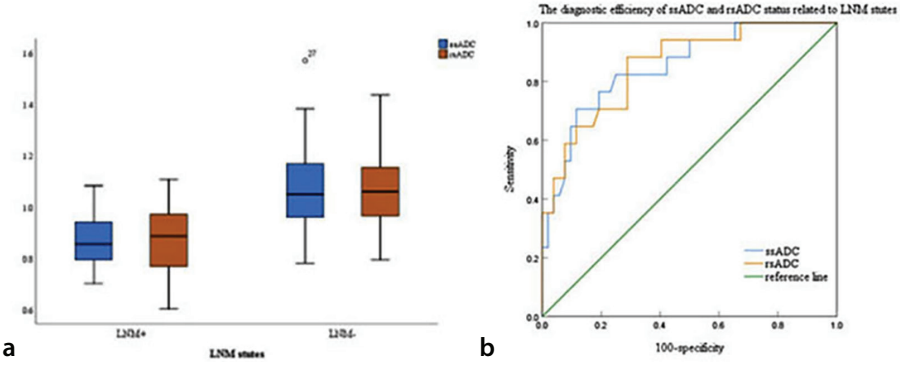

Figure 4. Plots **(a, b)** show boxplots of apparent diffusion coefficient values and receiver operating characteristic curves, respectively. ADC, apparent diffusion coefficient; LNM, lymph node metastasis.

Table 5. Diagnostic efficiency of apparent diffusion coefficient values in ss-EPI and rs-EPI with respect to LNM and LVSI status

ADC value ($\times 10^{-3}$ mm^2/s)	LNM status		P value	AUC	95% CI	LVSI status		P value
	LNM+ mean ± SD	LNM- mean ± SD				LVSI+ mean ± SD	LVSI- mean ± SD	
ssADC	0.87 ± 0.11	1.07 ± 0.16	0.000	0.851	0.744–0.925	0.99 ± 0.20	1.04 ± 0.13	0.271
rsADC	0.86 ± 0.14	1.07 ± 0.15	0.000	0.855	0.754–0.956	0.99 ± 0.21	1.05 ± 0.13	0.200

ADC, apparent diffusion coefficient; ssADC, apparent diffusion coefficient value of ss-EPI; rsADC, apparent diffusion coefficient value of rs-EPI; AUC, area under the receiver operating characteristic curve; LNM, lymph node metastasis; LVSI, lymphovascular space invasion; ss-EPI, single-shot echo-planar imaging; rs-EPI, readout-segmented echo-planar imaging; SD, standard deviation; CI, confidence interval.

radiotherapy without surgery or receiving neoadjuvant chemoradiotherapy prior to the surgery. Therefore, there were potential selection biases intrinsic to this retrospective single-center study. Second, the ROI in this study was delineated manually along the tumor margins on diffusion-weighted images. This approach may inadvertently introduce errors and deviations in determining tumor boundaries, and it is also notably time-consuming. Therefore, automated or semi-automated segmentation methods may represent a more efficient alternative. Future research should focus on enhancing comparative studies of these methods to develop a more effective research strategy. Third, although the evaluation of LVSI status in our study cohort was negative, we need to measure different ADCs (including tumor ADC, mini-ADC, and mini-ADC ratio) (32) and further estimate the relationship between ADC and LVSI status in large-cohort multicenter studies.

In conclusion, Over a similar scan time, rs-EPI significantly improves the qualitative image quality of DWI and has good diagnostic accuracy for LNM status in CC compared with conventional ss-EPI DWI, especially for the margin of CC lesions. However, neither could predict the LVSI status. Including rs-EPI DWI in routine clinical protocols for MRI may be a better choice.

Footnotes

Conflict of interest disclosure

The authors declared no conflicts of interest.

Funding

This study was supported by the Opening Project of Medical Imaging Key Laboratory of Sichuan Province (grant MIKLSP202106) and the popularization and application project of Chengdu Seventh People's Hospital-Chengdu Medical College joint scientific research (grant 2022LHIYPJ-03).

References

1. Bray F, Ferlay J, Soerjomataram I, Siegel RL, Torre LA, Jemal A. Global cancer statistics 2018: GLOBOCAN estimates of incidence and mortality worldwide for 36 cancers in 185 countries. *CA Cancer J Clin* . 2018;68(6):394-424. Erratum in: *CA Cancer J Clin*. 2020;70(4):313. [Crossref]
2. Padera TP, Kadambi A, di Tomaso E, et al. Lymphatic metastasis in the absence of functional intratumor lymphatics. Science. 2002;296(5574):1883-1886. [Crossref]
3. Bhatla N, Aoki D, Sharma DN, Sankaranarayanan R. Cancer of the cervix uteri. *Int J Gynaecol Obstet*. 2018;143(Suppl 2):22-36. [Crossref]
4. Koh WJ, Abu-Rustum NR, Bean S, et al. Cervical Cancer, Version 3.2019, NCCN Clinical Practice Guidelines in Oncology. *Natl Comp Canc Netw*. 2019;17(1):64-84. [Crossref]
5. Landoni F, Maneo A, Colombo A, et al. Randomised study of radical surgery versus radiotherapy for stage Ib-IIa cervical cancer. *Lancet*. 1997;350(9077):535-540. [Crossref]
6. Nathanson SD. Insights into the mechanisms of lymph node metastasis. *Cancer*. 2003;98(2):413-423. [Crossref]
7. Singh N, Arif S. Histopathologic parameters of prognosis in cervical cancer--a review. *Int J Gynecol Cancer*. 2004;14(5):741-750. [Crossref]
8. Wenkel E, Geppert C, Schulz-Wendtland R, et al. Diffusion weighted imaging in breast MRI: comparison of two different pulse sequences. *Acad Radiol*. 2007;14(9):1077-1083. [Crossref]
9. Porter DA, Heidemann RM. High resolution diffusion-weighted imaging using readout-segmented echo-planar imaging, parallel imaging and a two-dimensional navigator-based reacquisition. *Magn Reson Med*. 2009;62(2):468-475. [Crossref]
10. Qian W, Chen Q, Zhang Z, Wang H, Zhang J, Xu J. Comparison between readout-segmented and single-shot echo-planar imaging in the evaluation of cervical cancer staging. *Br J Radiol*. 2019;92(1094):20180293. [Crossref]
11. Zhang H, Huang H, Zhang Y, et al. Diffusion-weighted MRI to assess sacroiliitis: improved image quality and diagnostic performance of readout- segmented echo- planar imaging (EPI) over conventional single-shot EPI. *AJR Am J Roentgenol* .2021;217(2):450-459. [Crossref]
12. Viera AJ, Garrett JM. Understanding interobserver agreement: the kappa statistic. *Fam Med*. 2005;37(5):360-363. [Crossref]
13. Hallgren KA. Computing inter-rater reliability for observational data: an overview and tutorial. *Tutor Quant Methods Psychol*. 2012;8(1):23-34. [Crossref]
14. Xie M, Ren Z, Bian D, et al. High resolution diffusion-weighted imaging with readout segmentation of long variable echo-trains for determining myometrial invasion in endometrial carcinoma. *Cancer Imaging*. 2020;20(1):66. [Crossref]
15. Xia CC, Pu J, Zhang JG, et al. Readout-segmented echo-planar diffusion-weighted MR for the evaluation of aggressive characteristics of rectal cancer. *Sci Rep*. 2018;8(1):12554. [Crossref]
16. Thian YL, Xie W, Porter DA, Weileng Ang B. Readout-segmented echo-planar imaging for diffusion-weighted imaging in the pelvis at 3T-A feasibility study. *Acad Radiol*. 2014;21(4):531-537. [Crossref]
17. Friedli I, Crowe LA, Viallon M, et al. Improvement of renal diffusion-weighted magnetic resonance imaging with readout-segmented echo-planar imaging at 3T. *Magn Reson Imaging*. 2015;33(6):701-708. [Crossref]
18. Bogner W, Pinker-Domenig K, Bickel H, et al. Readout-segmented echo- planar imaging improves the diagnostic performance of diffusion-weighted MR breast examinations at 3.0 T. *Radiology*. 2012;263(1):64-76. [Crossref]
19. Yeom KW, Holdsworth SJ, Van AT, et al. Comparison of readout-segmented echo-planar imaging (EPI) and single-shot EPI in clinical application of diffusion-weighted imaging of the pediatric brain. *AJR Am J Roentgenol*. 2013;200(5):W437-W443. [Crossref]
20. Xu XQ, Liu J, Hu H, et al. Improve the image quality of orbital 3-T diffusion-weighted magnetic resonance imaging with readout-segmented echo-planar imaging. *Clin Imaging*. 2016;40(4):793-796. [Crossref]
21. Xu X, Wang Y, Hu H, et al. Readout-segmented echo-planar diffusion-weighted imaging in the assessment of orbital tumors: comparison with conventional single-shot echo-planar imaging in image quality and diagnostic performance. *Acta Radiol*. 2017;58(12):1457-1467. [Crossref]
22. Zhao M, Liu Z, Sha Y, et al. Readout-segmented echo- planar imaging in the evaluation of sinonasal lesions: a comprehensive comparison of image quality in single-shot echo-planar imaging. *Magn Reson Imaging*. 2016;34(2):166-172. [Crossref]
23. Moeller S, Yacoub E, Olman CA, et al. Multiband multislice GE-EPI at 7 tesla, with 16-fold acceleration using partial parallel imaging with application to high spatial and temporal whole-brain fMRI. *Magn Reson Med*. 2010;63(5):1144-1153. [Crossref]
24. Song SE, Woo OH, Cho KR, et al. Simultaneous multislice readout-segmented echo planar imaging for diffusion-weighted MRI in patients with invasive breast cancers. *J Magn Reson Imaging*. 2021;53(4):1108-1115. [Crossref]
25. Kenkel D, Barth BK, Piccirelli M, et al. Simultaneous multislice diffusion-weighted imaging of the kidney: a systematic analysis of image Quality. *Invest Radiol*. 2017;52(3):163-169. [Crossref]
26. Obele CC, Glielmi C, Ream J, et al. Simultaneous multislice accelerated free-breathing diffusion-weighted imaging of the liver at 3T. *Abdom Imaging*. 2015;40(7):2323-2330. [Crossref]
27. Taron J, Martirosian P, Kuestner T, et al. Scan time reduction in diffusion-weighted imaging of the pancreas using a simultaneous multislice technique with different acceleration factors: How fast can we go? *Eur Radiol*. 2018;28(4):1504-1511. [Crossref]

28. Huang H, Zhou M, Gong T, Wang Y. Feasibility of high-resolution readout-segmented echo-planar imaging with simultaneous multislice imaging in assessing rectal cancer. *Abdom Radiol (NY)*. 2023;48(7):2258-2269. [Crossref]
29. Byeon J, Kim JY, Cho AH. Readout-segmented echo-planar imaging in diffusion- weighted MR imaging of acute infarction of the brainstem and posterior fossa: comparison of single-shot echo-planar diffusion-weighted sequences. *Clin Imaging*. 2015;39(5):765-769. [Crossref]
30. Yao F, Huang M, Li J, Gao X. Yao F, Huang M, Li J, Gao X. Readout-segmented diffusion weighted imaging of the testis at 3.0 T: comparison with single-shot echo-planar imaging. *Abdom Radiol (NY)*. 2023;48(6):2131-2138. [Crossref]
31. Choi HJ, Kim SH, Seo SS, et al. MRI for pretreatment lymph node staging in uterine cervical cancer. *AJR Am J Roentgenol*. 2006;187(5):W538-W543. [Crossref]
32. Balleyguier C, Sala E, Da Cunha T, et al. Staging of uterine cervical cancer with MRI: guidelines of the European Society of Urogenital Radiology. *Eur Radiol*. 2011;21(5):1102-1110. [Crossref]
33. Williams AD, Cousins C, Soutter WP, et al. Detection of pelvic lymph node metastases in gynecologic malignancy: a comparison of CT, MR imaging, and positron emission tomography. *AJR Am J Roentgenol*. 2001;177(2):343-348. [Crossref]
34. Mi HL, Suo ST, Cheng JJ, et al. The invasion status of lymphovascular space and lymph nodes in cervical cancer assessed by mono-exponential and bi-exponential DWI-related parameters. *Clin Radiol*. 2020;75(10):763-771. [Crossref]
35. Li S, Liu J, Zhang F, et al. Novel T2 mapping for evaluating cervical cancer features by providing quantitative T2 maps and synthetic morphologic images: a preliminary study. *J Magn Reson Imaging*. 2020;52(6):1870-1871. [Crossref]
36. Li S, Zhang Z, Liu J, et al. The feasibility of a radial turbo-spin-echo T2 mapping for preoperative prediction of the histological grade and lymphovascular space invasion of cervical squamous cell carcinoma. *Eur J Radiol*. 2021;139:109684. [Crossref]
37. Zhang Q, Ouyang H, Ye F, et al. Multiple mathematical models of diffusion-weighted imaging for endometrial cancer characterization: correlation with prognosis- related risk factors. *Eur J Radiol*. 2020;130:109102. [Crossref]
38. Yang W, Qiang JW, Tian HP, Chen B, Wang AJ, Zhao JG. Minimum apparent diffusion coefficient for predicting lymphovascular invasion in invasive cervical cancer. *J Magn Reson Imaging*. 2017;45(6):1771-1779. [Crossref]
39. Cheng JM, Luo WX, Tan BG, Pan J, Zhou HY, Chen TW. Whole-tumor histogram analysis of apparent diffusion coefficients for predicting lymphovascular space invasion in stage IB-IIA cervical cancer.*Front Oncol*. 2023;13:1206659. [Crossref]
40. Otero-García MM, Mesa-Álvarez A, Nikolic O, et al. Role of MRI in staging and follow-up of endometrial and cervical cancer: pitfalls and mimickers. *Insights Imaging*. 2019;10(1):19. [Crossref]
41. Addley H, Moyle P, Freeman S. Diffusion-weighted imaging in gynaecological malignancy. *Clin Radiol*. 2017;72(11):981-990. [Crossref]